iScience

CellPress
OPEN ACCESS

Article

Targeting the PRC2-dependent epigenetic program alleviates urinary tract infections

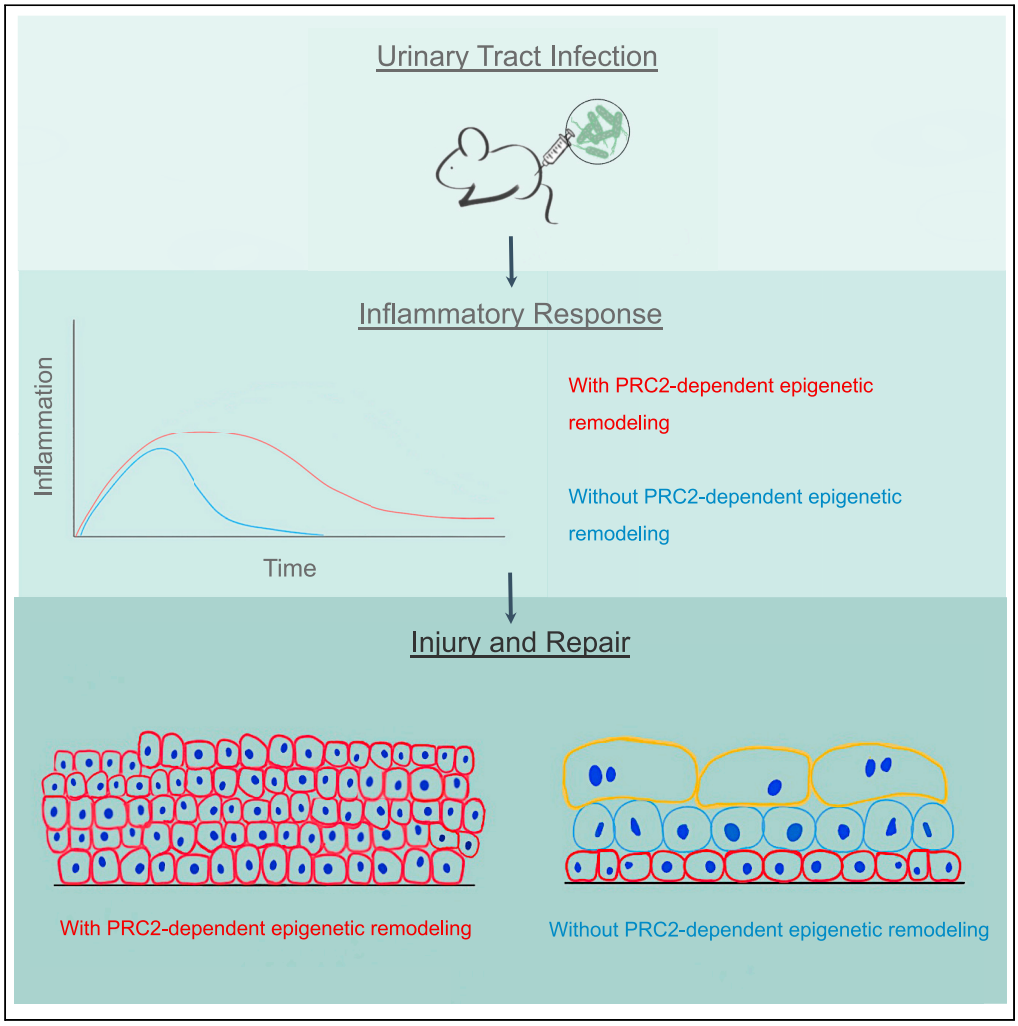

Chunming Guo, Mingyi Zhao, Xinbing Sui, ..., Christa M. Lam, Ping Zhu, Xue Li

sean.li@cshs.org

Highlights

UTI induces epigenetic remodeling of the bladder

The remodeling exacerbates inflammatory host response to subsequent infections

Targeting the PRC2-dependent epigenetic program reduces inflammatory damage

Ezh2 inhibitors therapeutically alleviate UTIs in mouse models

Guo et al., iScience 26, 106925
June 16, 2023
https://doi.org/10.1016/j.isci.2023.106925

iScience

CellPress
OPEN ACCESS

Article

Targeting the PRC2-dependent epigenetic program alleviates urinary tract infections

Chunming Guo,[1,2,5] Mingyi Zhao,[2,3,5] Xinbing Sui,[2,6] Zarine Balsara,[2,6] Songhui Zhai,[2] Michael Ahdoot,[4] Yingsheng Zhang,[1] Christa M. Lam,[1,2] Ping Zhu,[3] and Xue Li[1,2,7,*]

SUMMARY

Urinary tract infection (UTI) is a pervasive health problem worldwide. Patients with a history of UTIs suffer increased risk of recurrent infections, a major risk of antibiotic resistance. Here, we show that bladder infections induce expression of *Ezh2* in bladder urothelial cells. *Ezh2* is the methyltransferase of polycomb repressor complex 2 (PRC2)—a potent epigenetic regulator. Urothelium-specific inactivation of PRC2 results in reduced urine bacterial burden, muted inflammatory response, and decreased activity of the *NF-κB* signaling pathway. PRC2 inactivation also facilitates proper regeneration after urothelial damage from UTIs, by attenuating basal cell hyperplasia and increasing urothelial differentiation. In addition, treatment with Ezh2-specific small-molecule inhibitors improves outcomes of the chronic and severe bladder infections in mice. These findings collectively suggest that the PRC2-dependent epigenetic reprograming controls the amplitude of inflammation and severity of UTIs and that Ezh2 inhibitors may be a viable non-antibiotic strategy to manage chronic and severe UTIs.

INTRODUCTION

Urinary tract infections (UTIs) caused by uropathogenic *Escherichia coli* (UPEC) is a widespread public health issue that greatly decreases a patient's quality of life and poses a great financial burden. Patients with a prior history of bladder infection are at risk for subsequent UTIs and antibiotic resistance.[1–3] In the United States alone, cost to manage patients with UTI total to more than 3 billion dollars a year.[4,5] These reasons necessitate a deeper dive into the mechanisms underlying UTIs and exploration of alternatives to conventional antibiotic therapy.

In an acute bladder infection mouse model,[6] wild-type naive C57Bl/6 mice resolve from bacteriuria and bladder inflammation within days. If these mice are infected again, the second infection results in reduced urine bacterial count compared to the first infection.[7,8] However, if the second infection happens within 24 h, these mice—instead of having a self-limiting acute bladder infection—develop a superinfection that display severe urothelial damage, chronic cystitis, pyelonephritis, and even death.[9] Similarly, bladder injury followed by bacterial infection within 24 h also leads to a superinfection.[10] Superinfection is tightly associated with an exacerbated inflammatory host response and predisposes mice to chronic and recurrent UTIs.[11] Collectively, these findings suggest that bladder infection causes a lasting molecular change(s), such as mucosal imprint[12] and immunological memory,[7,8] that directly or indirectly influences clinical outcomes of UTIs. Nature of the lasting molecular changes induced by the infection, however, remains poorly understood.

Exposure to pathogens has been shown to induce epigenetic remodeling in host cells.[13–15] Epigenetic deposits such as histone H3 lysine 27 trimethylation (H3K27me3) have the potential to function as a molecular memory after pathogen clearance since they can persist through multiple cell cycles and several generations.[16–18] Human bladder urothelial carcinoma cells exposed to UPEC *in vitro* induce expression of *Ezh2,* the methyltransferase of polycomb repressor complex 2 (PRC2),[19] which catalyzes formation of H3K27me3. H3K27me3 is tightly linked to chromatin compaction and transcription silencing.[20–22] We have previously reported that the PRC2-dependent H3K27me3 modification plays a critical role in urothelial cell differentiation during bladder development.[23,24] PRC2 may also regulate the response of mature urothelial cells to UTIs—a possibility that has not yet been thoroughly explored.

[1]Samuel Oschin Comprehensive Cancer Institute, Department of Medicine, Department of Biomedical Sciences, Cedars-Sinai Medical Center, 8700 Beverly Blvd, Davis 3089, Los Angeles, CA 90048, USA

[2]Departments of Urology and Surgery, Boston Children's Hospital, Harvard Medical School, 300 Longwood Avenue, Boston, MA 02115, USA

[3]Guangdong Cardiovascular Institute, Guangdong Provincial Key Laboratory of Pathogenesis, Guangzhou Key Laboratory of Cardiac Pathogenesis and Prevention, Guangdong Provincial People's Hospital, Southern Medical University, Guangzhou, Guangdong 510100, China

[4]Department of Surgery, Cedars-Sinai Medical Center, 8700 Beverly Blvd, Davis 3089, Los Angeles, CA 90048, USA

[5]These authors contributed equally

[6]These authors contributed equally

[7]Lead contact

*Correspondence: sean.li@cshs.org

https://doi.org/10.1016/j.isci.2023.106925

Here, we provide *in vivo* evidence that *Ezh2* potentiates host inflammatory response after bladder infections. We show how phenotypically heightened inflammation, linked to poor UTI outcomes, may be driven by the PRC2-dependent epigenetic program. Moreover, we demonstrate that by targeting PRC2 activity (genetically and pharmacologically), we can limit excessive inflammation and pathological injuries from chronic and severe bladder infections. These findings suggest that the UTI-induced mucosal imprint is, in part, mediated by the PRC2-dependent epigenetic mechanism and targeting this underlying epigenetic program offers a non-antibiotic alternative to manage UTIs.

RESULTS

Bladder infection induces *Ezh2* expression in urothelial cells

To identify candidate UTI-induced epigenetic regulators, we performed a whole transcriptome analysis of the bladder urothelium at one day post-inoculation (1 dpi) of an UPEC strain UTI89 (Figure 1A and Table S1). In this acute infection model, *Ezh2* and *Suz12* were among the differentially expressed genes (DEGs) that were significantly upregulated (Figure 1B). Expressions of other members of the PRC2 complex (*Ezh1* and *Eed*) were not affected (Figure 1B), suggesting a gene-specific response to the infection. Quantitative analysis further confirmed a significant increase of *Ezh2* (Figure 1C). Since Ezh2 protein stability is also regulated by the proteosome degradation pathway,[25,26] we also examined Ezh2 protein level by immunofluorescent staining. At physiological conditions, Ezh2 protein was barely detectable in adult bladder urothelium (Figure 1D, PBS). After an acute infection, Ezh2 and H3K27me3 exhibited stronger immunoreactivity in the bladder urothelium and lamina propria (Figure 1D, 1 dpi). Together, these findings suggest that an acute bladder infection upregulates *Ezh2* gene transcription and/or protein stability.

In addition to *Ezh2*, other epigenetic regulators including genes that encode the DEAD-box-containing proteins Ddx26b and Ddx5, the SWI/SNF complex protein Smarcad1, and bromodomain protein Baz2b were upregulated as well (Table S1). Several long intergenic noncoding RNAs including *Xist*, *Neat1*, *A330044P14Rik*, *Gm21781*, *Al480526*, and *Gm26905* were significantly increased. Downregulated candidate epigenetic regulators included: *Chst2*, *Uchl1*, *Padi1*, *Padi2*, and *Inmt*. In this study, we focused on the PRC2-dependent epigenetic repression program due to its critical role in urothelial differentiation during bladder development.[23]

Inactivation of urothelial PRC2 dampens hyperproliferation caused by UTI

To examine a potential role of the PRC2-dependent epigenetic program in bladder infections, we used an urothelium-specific *Eed* conditional knockout mouse line (Eed^{cKO}), in which the PRC2-dependent methyltransferase activity mediated by both *Ezh1* and *Ezh2* was eliminated from the bladder urothelium.[23] Although urothelial progenitor lacking PRC2 activity displays a phenotype of precocious differentiation,[23] the mutant urothelium was grossly normal compared to heterozygous controls prior to the infection (Figures 1E–1I, PBS). A single dose of UTI89-inoculation caused noticeable urothelial damage at 1 dpi as indicated by the loss of cytokeratin 20-positive ($Krt20^+$) superficial cells and increase of $Krt5^+$ basal cells; the extent of these effects was also comparable between the mutants and controls (Figure 1E, 1 dpi). Similarly, $Krt20^+$ superficial cells were recovered within 3–7 days in both the mutants and controls. While Eed^{cKO} mutant responded to the bladder infection by activating urothelial cell proliferation, the cell proliferation rate in Eed^{cKO} mice was more than 2-fold (<30%) lower than controls (~60%) as indicated by Ki67 staining (Figures 1F and G, $p < 0.05$). Consistently, Eed^{cKO} urothelial cells had a 2-fold decrease of staining of a mitotic marker phosphohistone H3 (pHH3) compared to controls (Figures 1H and 1I, $p < 0.05$). Therefore, urothelium-specific inactivation of PRC2 dampens the hyperproliferative response to an acute bacterial infection.

PRC2 exacerbates inflammatory host response to bladder infection

Urine bacterial counts were significantly lower in urothelium-specific Eed^{cKO} mutant mice after an acute infection at 1 dpi (Figure 2A). Total intracellular bacterial communities (IBCs) formed per bladder at 3 or 6 h-post-inoculation (hpi) were comparable between controls and Eed^{cKO} (Figure 2B), implying that IBC formation was not affected in the mutants. Given that superficial cell exfoliation was comparable between mutants and controls (Figure 1), we next examined the potential impact of PRC2 on the inflammatory host response. Eed^{cKO} mutant bladders had fewer infiltrating immune cells (Figure 2C). Based on the degree of edema, urothelial damage, and immune cell infiltration,[27] Eed^{cKO} mice had nearly a 2-fold decrease in inflammation compared to controls (Figure 2D). To further examine the underlying mechanism, levels

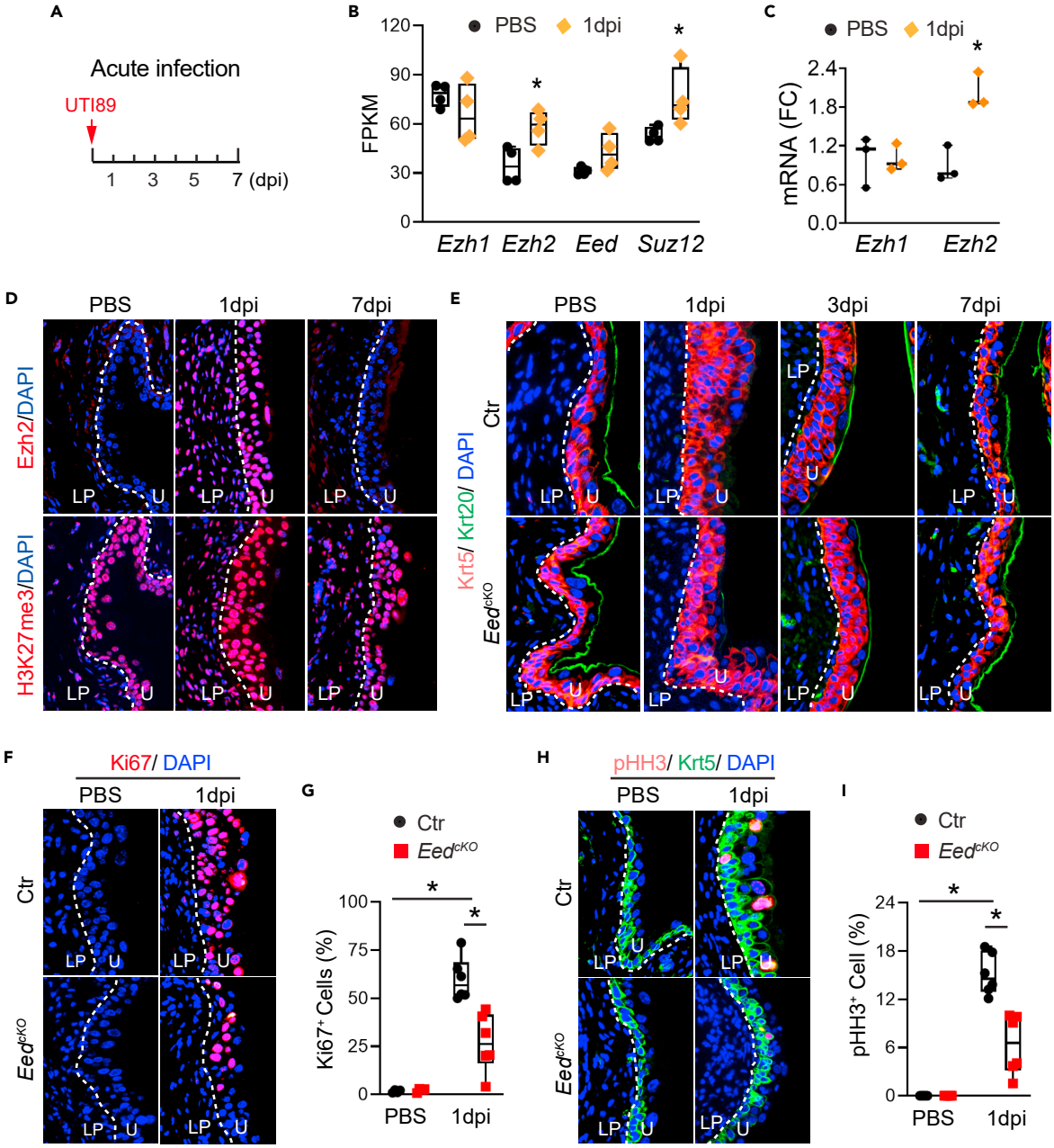

Figure 1. Acute infection induces *Ezh2* to promote hyperproliferation of urothelial progenitor cells

(A) Schematic of acute bladder infection using UPEC strain UTI89. dpi, day-post-inoculation.

(B) Expression levels of *Ezh1*, *Ezh2*, *Eed*, and *Suz12* in adult urothelium at 1 dpi of an acute infection. FPKM, fragments per kilobase of transcript per million mapped reads (n = 4).

(C) Quantitative RT-PCR confirmation of *Ezh1* and *Ezh2* expression levels in the bladder urothelium at 1 dpi. (n = 3) PBS-treated mice were used as uninfected controls. FC, fold change. (n = 3).

(D) Ezh2 (red) and H3K27me3 (red) immunostaining of wild-type mouse bladder sections at 1 and 7 dpi after UTI89 inoculation. PBS was used as an uninfected control. DAPI nuclear staining (blue); LP, lamina propria; U, urothelium; dashed lines demarcated the boundary between LP and U.

(E) Immunostaining of Eed^{cKO} versus control mouse bladder sections of mice at 1, 3, and 7 dpi using Krt5- (red) and Krt20 (green)-specific antibodies.

(F and G) Immunostaining of Ki67 (red)-specific antibodies and corresponding quantification at 1 dpi (Ctr, n = 4; Eed^{cKO}, n = 6).

(H and I) Immunostaining of pHH3- (red) and Krt5 (green)-specific antibodies and corresponding quantification at 1 dpi. (Ctr, n = 6; Eed^{cKO}, n = 6). Data represented as box and whisker plots with individual data points indicate third and first quartiles at upper and lower limits of the box respectively; the line within the box indicates the median, and the whiskers extend toward maximum and minimum values. Graphs with three points indicate maximum value, median, and minimum value (from top to bottom). Student's *t* test. *, $p < 0.05$.

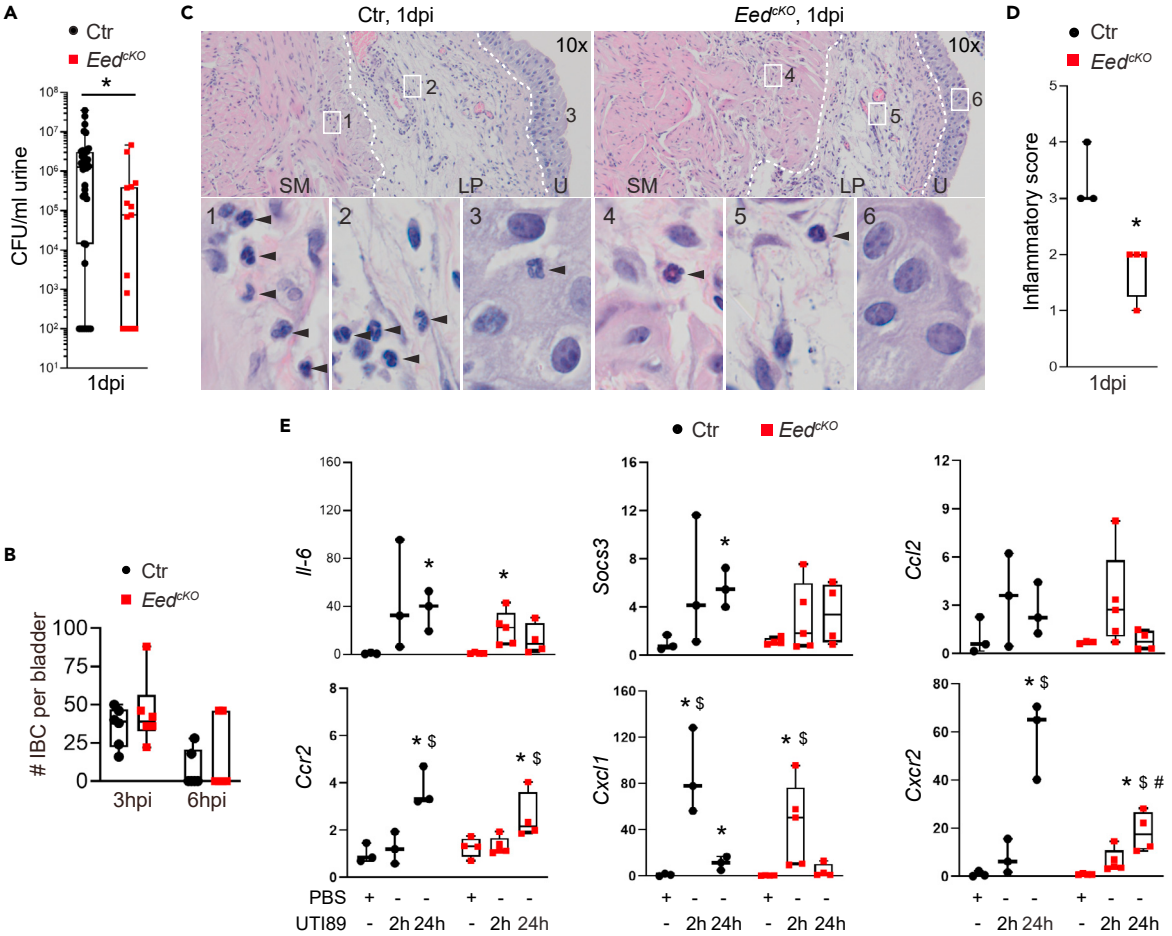

Figure 2. Genetic inactivation of PRC2 blunts host inflammatory response to an acute infection

(A) Box and whisker plot of urine bacterial counts represented by colony-forming units (CFU) per mL of urine at 1 dpi in controls (Ctr) and *Eed* knockouts with inactivated PRC2 (*Eed*^{cKO}), *p < 0.05, Mann-Whitney test (n ≥ 15).

(B) Counts of intracellular bacterial communities (IBCs) at 3 and 6 h-post-inoculation (hpi) (n = 6).

(C) H&E staining of bladder sections from heterozygous control (Ctr) and *Eed*^{cKO} at 1dpi of acute infection. Lamina propria (LP), smooth muscle (SM), and urothelium (U) layers are separated by dashed lines. Arrowheads, polymorphonuclear leukocytes.

(D) Inflammatory scores in controls and *Eed*^{cKO}. *, p < 0.05, Student's *t* test. (Ctr, n = 3; *Eed*^{cKO}, n = 4).

(E) Quantitative RT-PCR analysis of expression of inflammatory markers in controls and *Eed*^{cKO} mice bladders at 2 and 24 h (h) post-inoculation. *Gapdh* was used as an internal reference. y axis, fold change vs. controls; *, p < 0.05, UTI 2 or 24 h vs. PBS within the same genotype, unpaired Student's *t* test; $^{\#}$, p < 0.05, *Eed*^{cKO} vs. Ctr under the same treatment conditions, unpaired Student's *t* test; $^{\$}$, p < 0.05, vs. any other conditions within the same genotype, one-way ANOVA test (Ctr, n = 3; *Eed*^{cKO}, n ≥ 3).

of gene-specific transcription were quantitatively measured at 2 and 24 hpi to access the dynamic host response to an acute infection (Figure 2E). A significant upregulation of C-X-C motif chemokine ligand 1 *(Cxcl1)*/neutrophil-activating protein 3 (*NAP-3*) was observed in both controls and *Eed*^{cKO} mutants during early phase of infection at 2 hpi. Similarly, *Il-6*, chemokine (C-C motif) receptor 2 (*Ccr2*), and chemokine (C-X-C motif) receptor 2 (*Cxcr2*) were significantly induced in both mutants and controls later at 24 hpi. While significantly high levels of *Cxcl1*, *Cxcr2*, and suppressor of cytokine signaling-3 were observed in controls, expression levels of these genes were apparently lower in the mutants. In particular, *Cxcr2* expression was significantly lower in the mutants than in controls at 24 hpi. Collectively, these observations suggest that *Eed*^{cKO} mutant mice develop a less exaggerated inflammatory host response and resolve from infection more effectively than controls.

Bladder infection results in a rapid nuclear accumulation of *NF-κB* first in superficial cells and subsequently, in intermediate and basal cells.[28] To understand how PRC2 affects inflammation, we examined *NF-κB*

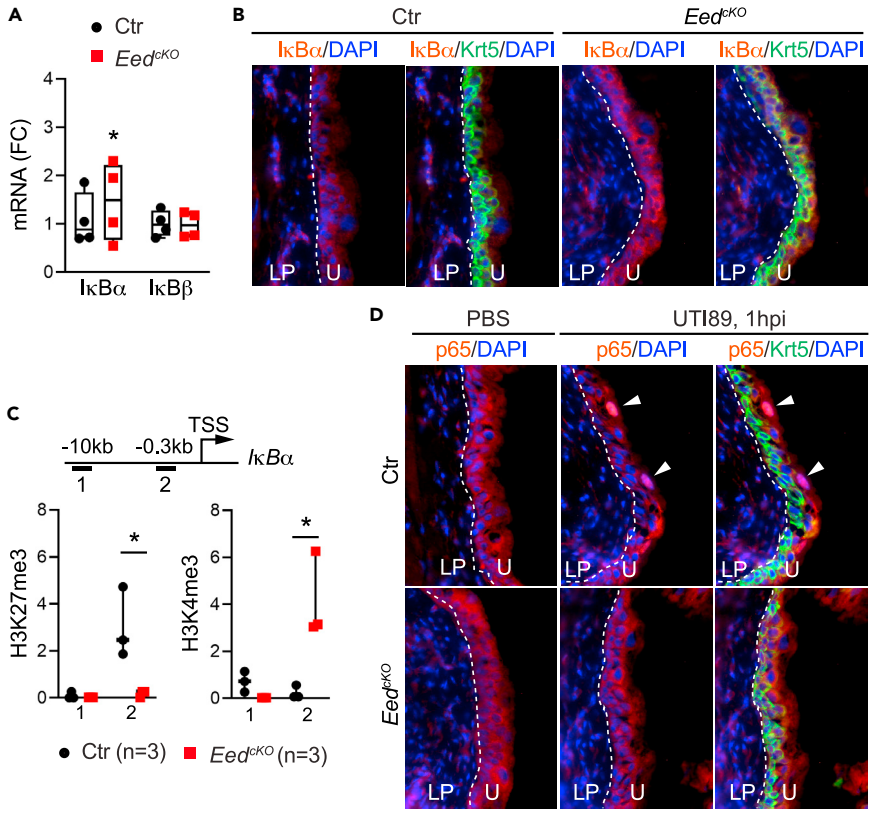

Figure 3. PRC2 promotes the *NF-κB* signaling pathway in bladder urothelium

(A) Quantitative RT-PCR analysis of *IκBα* and *IκBβ* mRNAs in bladder urothelium of heterozygous (Ctr, n = 4) and *Eed*^{cKO} mice (n = 4). *Gapdh* was used as an internal reference. FC, fold change.

(B) Immunostaining of IκBα (red) and Krt5 (green) of control and *Eed*^{cKO} mice bladder sections. LP, lamina propria; U, urothelium.

(C) Chromatin immunoprecipitation (ChIP) assay of *IκBα* locus (schema) using H3K27me3-and H3K4me3-specific antibodies. TSS, transcription start site (n = 3); y axis, percentage of input.

(D) Immunostaining of RelA/p65 subunit of NF-κB (red) and Krt5 (green) of control and *Eed*^{cKO} mice bladder sections at 1 hpi. DAPI nuclear counter staining (blue); PBS, phosphate buffered saline; White arrowheads, nuclear localized RelA/p65. Data in A and C represented as box and whisker plots. *, $p < 0.05$, Student's *t* test.

activation and found that expression of *IκBα* was significantly upregulated in the bladder urothelium of *Eed*^{cKO} mutants (Figure 3A). Consistently, anti-IκBα immunoreactivity was markedly stronger in *Eed*^{cKO} mice compared to controls (Figure 3B). Chromatin immunoprecipitation further showed that the occupancy of repression histone mark H3K27me3 was significantly reduced, while the epigenetic activation mark H3K4me3 was significantly enriched at the *IκBα* promoter region of *Eed*^{cKO} mice (Figure 3C). Furthermore, much fewer superficial cells with positive nuclear staining of RelA/p65, a component of *NF-κB* protein dimer, were observed in *Eed*^{cKO} mice compared to controls at 1 hpi (Figure 3D). Taken together, these findings suggest that in an acute bladder infection, urothelium-specific inactivation of PRC2 attenuates a potentially overreactive inflammatory host response and enhances resolution of inflammation through the *NF-κB*-dependent mechanism.

Eed^{cKO} mice are resistant to chronic bladder infections

Based on our results from the acute bladder infection model, we hypothesized that *Eed*^{cKO} mice are protected against injuries from chronic or repeated bladder infections. To test the hypothesis, we inoculated mice with UTI89 7 times with a 7-day convalescence after each inoculation to model chronic infections in C57Bl/6 mice (Figure 4A). At the first inoculation, control mice developed severe bacteriuria with approximately 10^6 colony-forming units (CFU) of bacteria in the urine at 1 dpi (Figure 4B, 1x UTI, Ctr), similar to what was observed in Figure 2A. Compared to controls, *Eed*^{cKO} mice had significantly lower urine bacterial counts at 1 dpi after 1x UTI (Figure 4B, 1x UTI, *Eed*^{cKO}). Bladder infection was largely resolved in the mutant

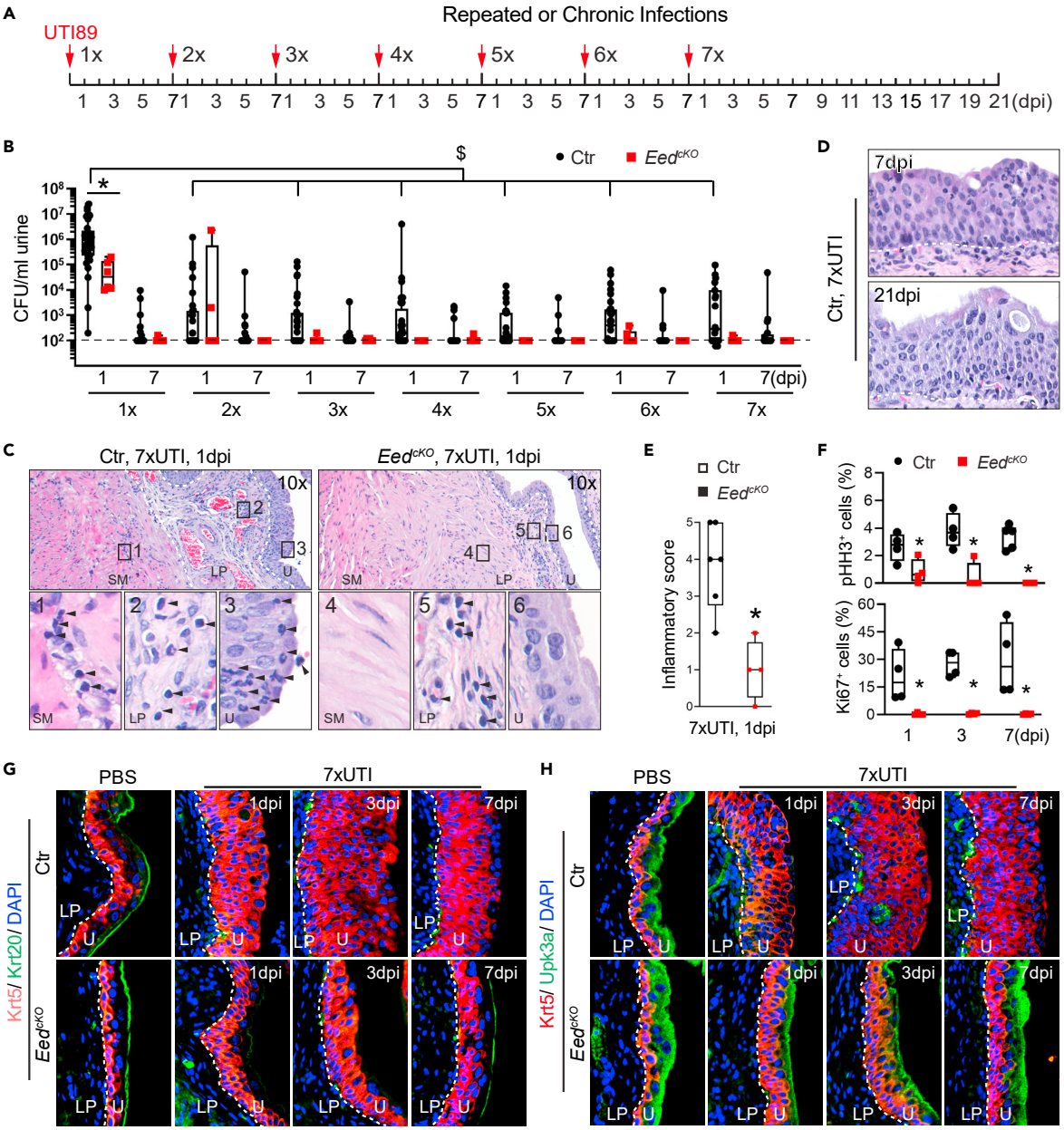

Figure 4. Urothelium-specific PRC2 inactivation attenuates inflammatory host response to repeated or chronic bladder infections

(A) Schematic diagram of repeated infection. dpi, day-post-inoculation.

(B) Urine bacterial counts represented by colony-forming units (CFU) per mL of urine from 1 to 7 infections. *p < 0.05, Mann-Whitney test. (Ctr, n ≥ 17; *Eed*^{cKO}, n = 6).

(C) H&E staining of bladder sections from heterozygous control (Ctr) and *Eed*^{cKO} mice after the seventh infection (7XUTI) at 1 dpi. LP, lamina propria; U, urothelium; SM, smooth muscle. Arrowheads, polymorphonuclear leukocytes.

(D) Heterozygous control mice after the seventh infection (7XUTI) at 7 and 21 dpi, indicating a lasting impact of C^{+}UTI superinfection on the urothelium.

(E) Inflammatory scores. (Ctr, n = 6; *Eed*^{cKO}, n = 4).

(F) Quantification of cell proliferation rates based on numbers of pHH3- and Ki67-positive cells. (Ctr, n ≥ 4; *Eed*^{cKO}, n ≥ 3).

(G and H) Immunostaining of Krt5 (red), Krt20 (green), and Upk3a (green) of bladder sections of control and *Eed*^{cKO} mice after 7XUTI. DAPI nuclear counter staining (blue). Data in E and F represented as box and whisker plots. *, p < 0.05, Student's *t* test.

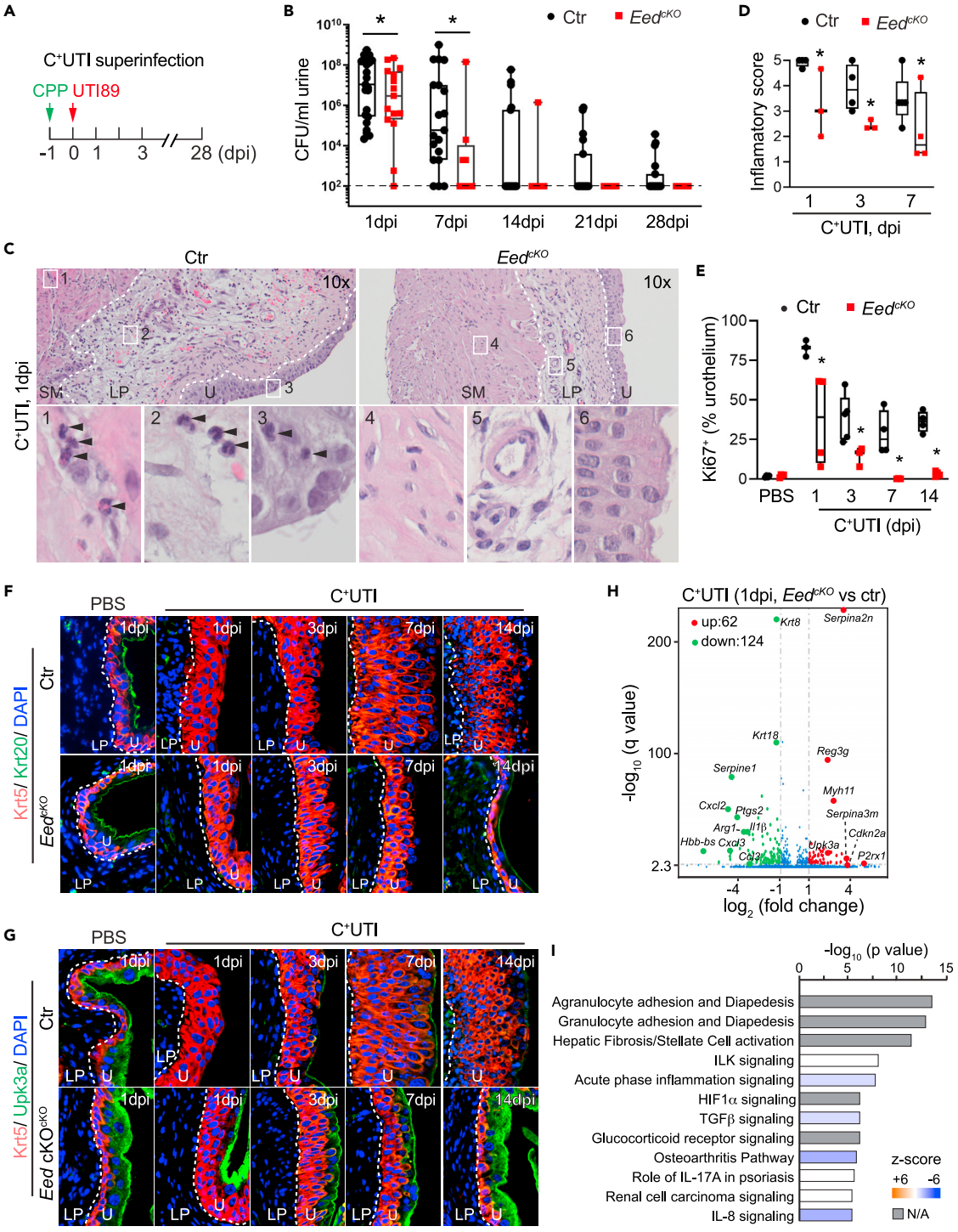

Figure 5. Urothelium-specific inactivation of PRC2 attenuates inflammatory host response to C⁺UTI superinfection

(A) Schematic diagram of C⁺UTI superinfection. dpi, day-post-inoculation.

(B) Prospective urine bacterial counts represented by colony-forming units (CFU) per mL of urine of heterozygous control (Ctr) and *Eed*^{cKO} mice after C⁺UTI superinfection. *p < 0.05, vs. Ctr, Mann-Whitney test. (Ctr, n ≥ 19; *Eed*^{cKO}, n ≥ 9).

(C) H&E staining of bladder sections from heterozygous control (Ctr) and *Eed*^{cKO} mice bladder sections at 1 dpi after C⁺UTI superinfection. LP, lamina propria; SM, smooth muscle; U, urothelium. Arrowheads, polymorphonuclear leukocytes.

(D) Inflammatory scores. (Ctr, n ≥ 4; *Eed*^{cKO}, n ≥ 3).

(E) Quantification of cell proliferation rates based on numbers of Ki67+ cells. (Ctr, n ≥ 3; *Eed*^{cKO}, n ≥ 3).

Figure 5. *Continued*

(F and G) Immunostaining of Krt5 (red), Krt20 (green), and Upk3a (green) of bladder sections of control and Eed^{cKO} mice after C^+UTI superinfection. DAPI nuclear counter staining (blue).

(H) Differential expressed genes in bladder urothelium between Eed^{cKO} and Ctr at 1 dpi of C^+UTI superinfection. q-value ≤ 0.05, fold change ≥ 2. (n = 2).

(I) Top pathways of the DEGs predicted by Ingenuity Pathway Analysis. Data in D and E represented as box and whisker plots. *, $p < 0.05$, Student's *t* test.

at 7 dpi but only partially resolved in heterozygous control mice (Figure 4B, 7 dpi of 1x UTI). Repeated infections caused milder bacteriuria (Figure 4B, 2–7x UTIs, Ctr, $p < 0.05$), consistent with previous reports that C57Bl/6 mice can self-resolve acute bladder infection and, moreover, that the infection elicits partial immunological protection against subsequent infections.[7,8,29–31] Unlike controls, bacteriuria was nearly absent in the mutants after repeated infections (Figure 4B, 3–7x UTIs, 1 and 7 dpi).

Chronic infections caused severe urothelial hyperplasia in control mice and a hyperplastic phenotype that lasted for more than 21 days after the seventh infection (Figures 4C and 4D, Ctr). In Eed^{cKO} mice, however, this urothelial hyperplasia phenotype was not observed (Figure 4C, Eed^{cKO}). The inflammatory score was also significantly lower in Eed^{cKO} bladders than controls (Figure 4E). Consistent with the hyperplasia phenotype in control mice, high levels of cell proliferation—as indicated by both Ki67 and pHH3 immunostaining (Figures 4F and S1A)—were observed only in control but not in Eed^{cKO} mice. $Krt20^+$ superficial cells were lost and not regenerated among control mice after repeated infections (Figure 4G). Instead, $Krt5^+$ basal cells expanded and occupied the entire thickness of bladder urothelium in controls (Figure 4H), suggesting that repeated infections caused exfoliation of both intermediate and superficial cells and failure to regenerate. While exfoliation of $Krt20^+$ superficial cells also occurred in Eed^{cKO} at 1 and 3 dpi after the seventh infection, regeneration was observed at 7 dpi in Eed^{cKO}. Moreover, repeated infections appeared to have minimal impact on Upk3a immunoreactivity of Eed^{cKO} mutants (Figure 4G), suggesting that $Krt20^-$/$Upk3^+$ intermediate cells were maintained during repeated infections in Eed^{cKO} mice. Collectively, these findings suggest that Eed^{cKO} mice are more resistant to repeated infections than controls.

Genetic inactivation of PRC2 improves outcomes of a bladder superinfection

To examine whether Eed^{cKO} mice could be protected from a superinfection, we inoculated Eed^{cKO} mice with UTI89 one day after a cyclophosphamide (CPP)-induced bladder injury[10]; we refer to this bladder superinfection model as C^+UTI superinfection (Figure 5A). Heterozygous control mice superinfected with C^+UTI developed severe bacteriuria that persisted for more than four weeks (Figure 5B). Eed^{cKO} mice, on the other hand, had significantly lower urine bacterial burden at 1 dpi, and bacteriuria was largely cleared within two weeks (Figure 5B). Histological analysis demonstrated that control mice developed apparent edema, severe urothelial damage, and basal cell hyperplasia at 1 dpi of C^+UTI (Figure 5C). High levels of immune cell infiltration were also observed in control bladders. In contrast, Eed^{cKO} mice demonstrated less urothelial hyperplasia, edema, and immune cell infiltration, resulting in a lower inflammatory score compared to control mice (Figure 5D). Cell proliferation rates were also significantly lower in Eed^{cKO} mice than controls (Figures 5E and S1B). Eed^{cKO} mice sustained a similar level of initial urothelial damage as control mice, observed by comparable exfoliation levels of $Krt20^+$ superficial cells at 1 and 7 dpi (Figure 5F). However, expression of *Krt20* reemerged at 14 dpi in Eed^{cKO} but not in controls, indicating that knockouts had better recovery than controls (Figure 5F). Eed^{cKO} mice also maintained *Upk3a* gene expression after C^+UTI superinfection (Figure 5G), which was not observed in control mice. Instead, the urothelium of control mice consisted entirely of $Krt5^+$ basal cells (Figures 5F and 5G), similar to controls with repeated bladder infections (Figure 4). Collectively, these findings suggest that Eed^{cKO} mice are better protected from a superinfection than controls.

To understand the mechanism underlying the PRC2-dependent host response to C^+UTI superinfection, we performed a whole-genome transcriptomic analysis of the urothelium of superinfected bladders. A total of 186 DEGs were identified between Eed^{cKO} and control mice at 1dpi of C^+UTI (Figure 5H). Among them, 124 genes were significantly downregulated and 62 genes were upregulated in Eed^{cKO} mice when compared to controls. A list of inflammatory markers including *Cxcl2*, *Cxcl3*, *Ccl2*, *Ccl3*, *Il-1β*, *Il-11*, and *Ptgs2* (aka *Cox2*) were downregulated in Eed^{cKO} mice; this is consistent with the observed decrease in inflammatory score. Particularly noteworthy were suppression of *Cox2* because mice treated with Cox2 inhibitors significantly reduce chronic cystitis.[32] Ingenuity Pathway Analysis of DEGs further predicted the top 10 affected canonical pathways (Figure 5I), including acute phase inflammation and *Il-8* neutrophil chemotaxis pathways which were significantly reduced in Eed^{cKO} mice. Collectively, these findings strongly suggest that the PRC2-dependent epigenetic program in the bladder urothelium exacerbates the inflammatory host response, causing severe urothelial damage and poor outcomes to a bladder superinfection.

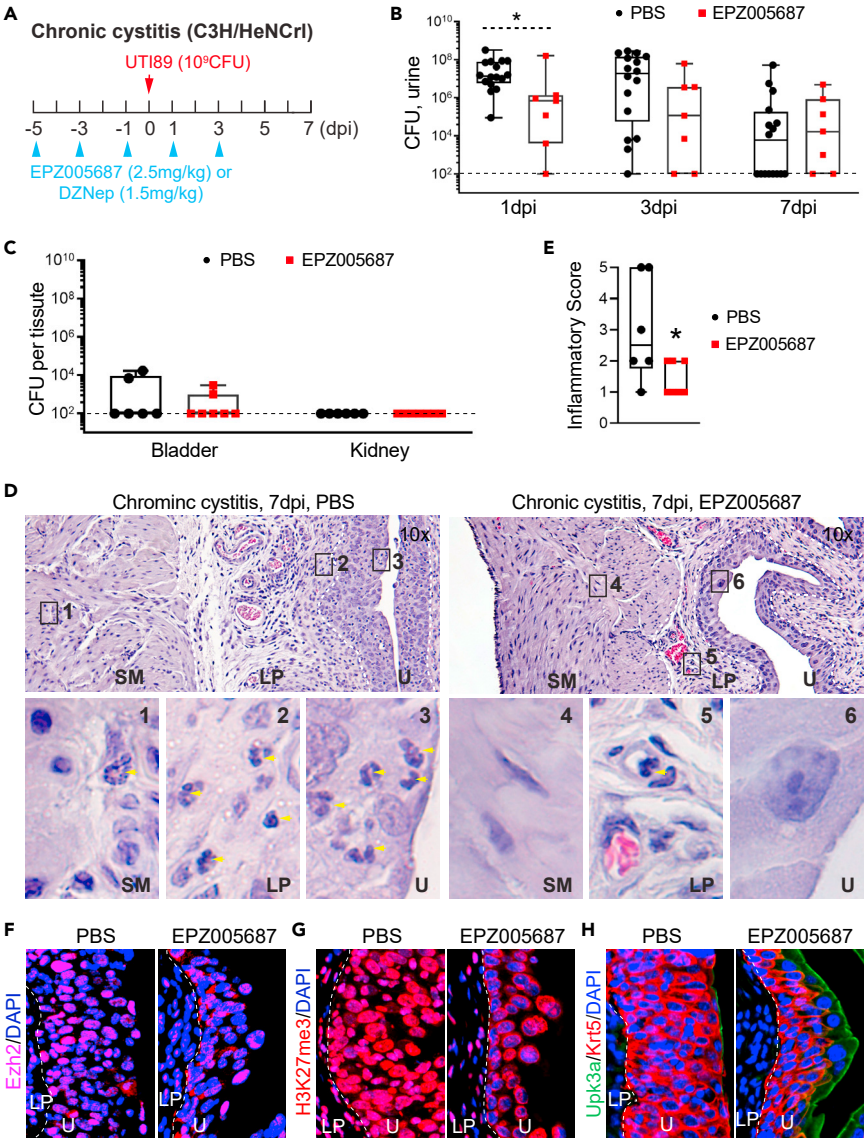

Figure 6. Pretreatment with Ezh2-specific inhibitor improves outcomes of chronic cystitis

(A) Schematic diagram of Ezh2-specific inhibitor (EPZ005687) or DZNep treatment of chronic cystitis.

(B) Bacterial counts in the urine after vehicle control (PBS) or EPZ005687 treatment. *$p < 0.05$, Mann-Whitney test. (PBS, n = 20; EPZ005687, n = 7).

(C) Bacterial counts in the bladder and kidney after PBS or EPZ005687 treatment at 7 dpi. (PBS, n = 6; EPZ005687, n = 7).

(D) H&E staining of bladder sections of wild-type C3H/HeNCrl mice at 7 dpi of chronic cystitis. LP, lamina propria; U, urothelium; SM, smooth muscle. Yellow arrowheads, polymorphonuclear leukocytes.

(E) Inflammatory score at 7 dpi. *$p < 0.05$, Student's *t* test. (PBS, n = 6; EPZ005687, n = 7).

(F–H) Immunostaining of Ezh2 (pink), H3K27me3 (red), Upk3a (green), and Krt5 (red) of bladder sections from mice with chronic cystitis after PBS or EPZ005687 treatment. DAPI nuclear counter staining (blue).

Ezh2-specific inhibitor improves outcomes of preclinical models of UTIs

Chronic bladder infection is a major health issue and is also associated with increased bladder cancer risk in humans.[33] We therefore examined effects of Ezh2 inhibition on a preclinical model of chronic cystitis using C3H/HeN mouse strain[11,12,32] (Figure 6A). EPZ005687 (EPZ) is an Ezh2-specific small-molecule inhibitor.[34] EPZ alone had minimal effects on bacterial counts in the bladder and kidneys, although bacteriuria was moderately lower at 1 dpi (Figures 6B and 6C). However, EPZ treatment dramatically decreased urothelial hyperplasia phenotype and inflammatory score (Figures 6D and 6E): an indication of reduced inflammatory

host response. EPZ also blunted *Ezh2* induction and decreased H3K27me3 level in bladder urothelial cells (Figures 6E–6G). Furthermore, EPZ-treated mice exhibited a much milder basal cell hyperplasia phenotype and maintained expression of a terminal differentiation marker *Upk3a* (Figure 6H). DZNep, a non-specific Ezh2 inhibitor,[35] exhibited a potent Ezh2 inhibition and reduction of H3K27me3 in the bladder (Figure S2A). It also mildly decreased urine bacterial counts (Figure S2B) but markedly attenuated bladder edema and urothelial hyperplasia (Figure S2C). Neutrophil infiltration and inflammatory score were significantly lower in DZNep- than PBS-treated mice (Figure S2D). High levels of *Upk3a* expression were also detected in DZNep-treated but not PBS-treated mice (Figure S2E). Taken together, these findings suggest that *Ezh2* inhibitors decrease inflammation and urothelial hyperplasia, thereby improving outcomes of chronic cystitis.

Consistent with the observation that EPZ attenuates inflammation (Figure 6), we found that mice treated with EPZ had fewer superficial cells with nuclear RelA/p65 staining compared to vehicle controls at 1 hpi of an acute bladder infection (Figure 7A). To ascertain whether the effect was mediated directly by urothelial cells independent of immune cells, mouse bladder organoids were differentiated into $Krt20^+$ superficial and $Krt5^+$ basal cells (Figure S3A).[36] UTI89 exposure of the cultured urothelial cells induced a robust nuclear translocation of RelA/p65, which was blocked by EPZ pretreatment (Figure S3A). Therefore, Ezh2 inhibition specifically attenuates the innate inflammatory response of bladder urothelial cells to UPEC.

Next, we explored the effect of Ezh2 small-molecule inhibitors in a severe superinfection model (C^+UTI superinfection). Mice were sequentially treated with: (1) three doses of EPZ, (2) CPP and UTI89 (*i.e.,* C^+UTI), and finally (3) 2 doses of EPZ (Figure 7B). EPZ treatment did not affect UPEC growth or viability *in vitro*, nor bacterial counts in the bladder or kidneys (Figure 7C). It did, however, decrease bacteriuria at 3 dpi of C^+UTI superinfection. Histological analysis further demonstrated that EPZ-treated bladders had much fewer immune cell infiltration as reflected by the reduced inflammatory score (Figures 7D and 7E), consistent with its role in reducing inflammation. Urothelial cell proliferation was also significantly reduced in EPZ-treated mice (Figure 7F). Furthermore, expression of urothelial cell differentiation marker *Upk3a* was preserved in EPZ but not control mice (Figure 7G). Like EPZ, DZNep reduced H3K27me3 levels in the bladder at 7 dpi in the C^+UTI superinfection model (Figure S3B). DZNep reduced bacterial counts in the urine (Figure S3C) but not in the bladder and kidneys (Figure 3D). DZNep-treated mice displayed fewer infiltrating neutrophils, mild basal hyperplasia, blunted expression of *Ezh2*, and increased expression of *Upk3a* and *Krt20* (Figures S3F–S3I). Collectively, these findings demonstrate therapeutic viability of Ezh2 inhibitors in preclinical models of bladder infections.

DISCUSSION

This study uncovers a previously unknown role of the PRC2-dependent epigenetic reprograming in regulating the inflammatory host response to bacterial infections in the bladder. Findings suggest that the bacteria-induced epigenetic remodeling of the bladder urothelium exacerbates inflammation and urothelial injury, leading to poor outcomes in acute, chronic, and severe bladder infections. Findings here further suggest a possible non-antibiotic therapeutic strategy to ameliorate chronic and severe UTIs by targeting the underlying PRC2-dependent epigenetic program.

UPEC induces expression of multiple epigenetic regulators in the bladder. Among them, *Ezh2* is significantly upregulated in both the bladder urothelium and underlying mesenchymal cells. While we cannot rule out contributions from immune and mesenchymal cells, we show evidence that the PRC2-dependent epigenetic program in urothelial cells plays a critical role in promoting the inflammatory host response to bladder infections. *Ezh2* induction is tightly linked to increased expression of inflammatory cytokines and chemokines, severe basal cell hyperplasia, and impaired urothelial cell terminal differentiation. While the underlying mechanism of PRC2-mediated inflammatory response in the bladder remains to be defined, our findings suggest that it promotes the NF-κB signaling pathway by epigenetic repression of the *IκBα* locus. Indeed, the UTI-induced NF-κB activation, as indicated by RelA/p65 nuclear translocation, is markedly reduced in Eed^{cKO} mice. In addition to the PRC2-dependent histone methylation, *Ezh2* may also function in the methyltransferase-independent manner to enhance *NF-κB* activity.[37] It is worth noting that *NF-κB* directly regulates *Ezh2* expression in human fibroblasts,[38] suggesting that feedback regulation between *Ezh2* and *NF-κB* molecular pathways may exacerbate and prolong the inflammatory host response to bladder infections. An exacerbated inflammatory host response is characterized by uncontrolled inflammation and tissue damage that ultimately weakens the host immune efficacy against present and future

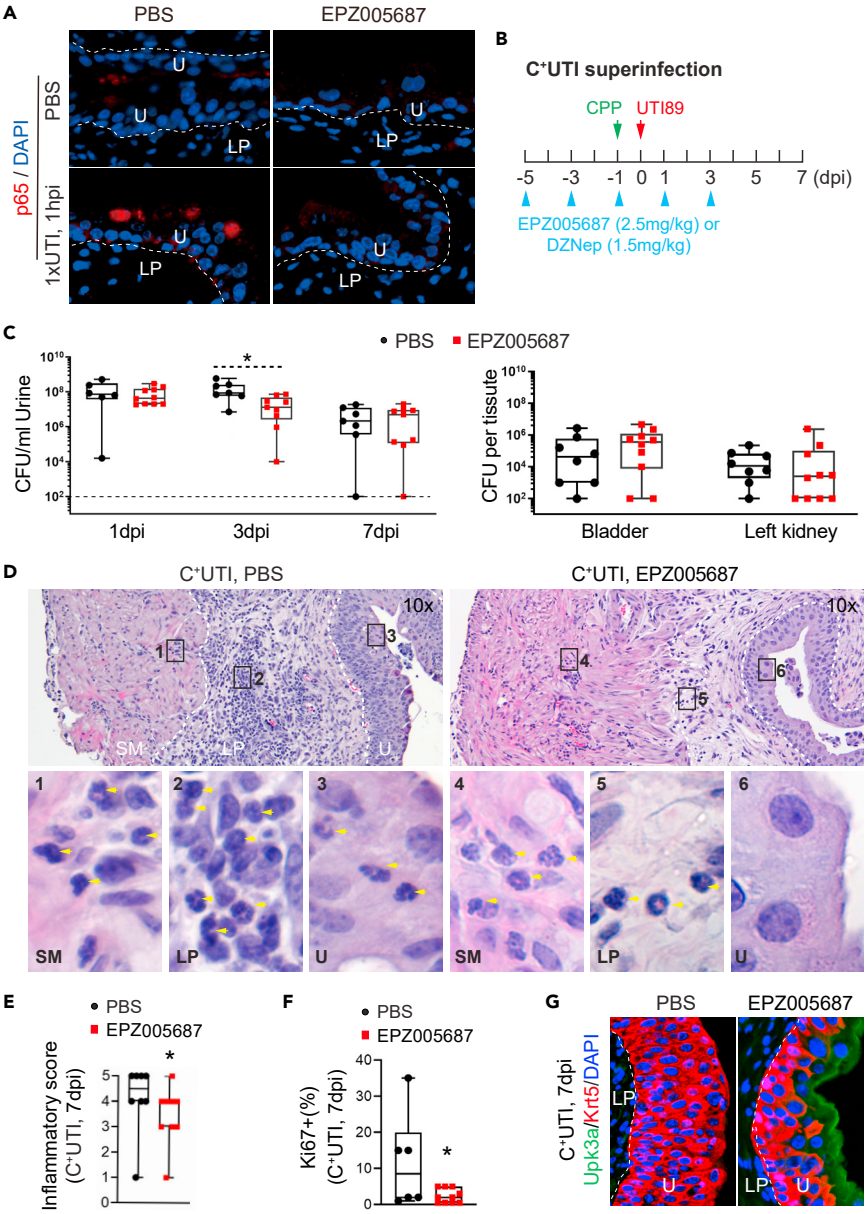

Figure 7. Pretreatment with Ezh2-specific inhibitor improves outcome of C$^+$UTI superinfection

(A) Immunostaining of nuclear translocation of RelA/p65 (red) in bladder sections of wild-type C57Bl6/J mice from acute infection with or without EPZ005678 treatment at 1 hpi; negative control of acute infection (PBS). DAPI nuclear count staining (blue); LP, lamina propria; U, urothelium.

(B) Schematic diagram of Ezh2-specific inhibitor (EPZ005687) or DZNep treatment of C$^+$UTI superinfection.

(C) Bacterial counts in the urine and tissues (bladder and kidneys) of C57Bl/6 mice after C$^+$UTI superinfection with or without EPZ005678 treatment. *$p < 0.05$, Mann-Whitney test. (PBS, $n \geq 6$; EPZ005687, $n \geq 9$).

(D) H&E staining of bladder sections of wild-type C57Bl/6J mice at 7 dpi of C$^+$UTI superinfection. SM, smooth muscle; arrowheads, polymorphonuclear leukocytes.

(E) Inflammatory scores. (PBS, n = 8; EPZ005687, n = 10).

(F) Percentage of Ki67$^+$-proliferating cells in bladder urothelium with or without EPZ005678 treatment after C$^+$UTI superinfection at 7 dpi. (PBS, n = 6; EPZ005687, n = 10).

(G) Immunostaining of Upk3a (green) and Krt5 (red) of bladder sections of mice at 7 dpi of C$^+$UTI superinfection after EPZ005687 treatment. DAPI nuclear counter staining. Data in E and F represented as box and whisker plots. *, $p < 0.05$, Student's *t* test.

bacterial infections. Importantly, small-molecule Ezh2 inhibitors significantly diminished bladder inflammatory responses to chronic and severe infections. While the design of this study could not differentiate the prophylactic and therapeutic effects, these findings provide proof-of-concept evidence that targeting the PRC2-dependent epigenetic program offers a non-antibiotic adjuvant strategy to treat UTIs.

Epigenetic reprograming has been linked to the trained immunity-like inflammatory memory in epithelial cells including the skin and airway epithelial progenitors.[39,40] However, epigenetic repression in modulating inflammatory host response to bacterial infections in the bladder has not been reported. Given the quiescent nature of bladder urothelium[24] and how the PRC-dependent H3K27me3 modification persists through cell cycles and generations,[18,35] we speculate that the PRC2-dependent epigenetic reprograming has a lasting impact on the pathophysiology of the bladder urothelium. The virulence factor α-hemolysin is required to attenuate host Akt/protein kinase B signaling pathway during UPEC infection.[41] In an α-hemolysin-dependent manner, UPEC also abrogates global histone H3 and H4 acetylation in Sertoli cells to promote cell survival.[42] In addition to α-hemolysin, other pore-forming bacterial toxins have been reported to mediate dephosphorylation of histone H3 and deacetylation of histone H4[13]. Hultgren and colleagues have previously shown that a primary bladder infection leaves behind a molecular imprint on the bladder tissue that lasts for more than seven months and, importantly, sensitizes recurrent infections.[12] It is possible that a UTI-induced mucosal imprint is, in part, mediated by the PRC2-dependent epigenetic program.

Changes made after past infections often arm an organism to be better prepared upon subsequent encounters. Vertebrates have a highly specialized adaptive immune system, which produces long-lasting immunological memory and enhanced responses to eliminate pathogens. Emerging evidence suggests that innate immune cells also display a long-term enhanced inflammatory response, termed trained immunity,[43] to challenge infections, suggesting that mammalian cells may have retained an ancestral mechanism of immunological memory to defend against infections.[44,45] While epithelial cells provide first-line defense against pathogens, it has been poorly understood whether mammalian epithelial cells develop memory from past pathogen encounters to better respond during a secondary infection. Future studies are needed to ascertain whether mucosal imprint and trained immunity share a similar underlying epigenetic mechanism.

The PRC2-dependent inflammatory response in urothelial progenitor cells appears to hinder terminal differentiation of superficial cells. Loss of the superficial cell layer grants the invading pathogens access to deeper bladder tissue and predisposes the host to chronic cystitis.[46] While the UTI-induced epigenetic memory in urothelial cells accelerates bacterial clearance by a heightened inflammatory response, it also increases the risk of chronic infection due to the impaired urothelial homeostasis. UPEC have evolved to subvert the host's defense through multiple strategies,[47] including intracellular localization,[46,48,49] filamentation,[50] attenuation of cytokine production,[51–53] killing of natural killer cells,[54] limiting antigen presentation,[8] and promoting cell survival.[42] Our findings provide evidence that additionally, UPEC uses the epigenetic remodeling of urothelial cells to benefit pathogens in the bladder.

Injuries awaken the quiescent bladder urothelium, causing urothelial progenitor cell proliferation and differentiation to repair the damage.[24] UTI-induced *Ezh2* expression coincides with reactivation of the cell cycle of urothelial progenitor cells. The basal cell proliferation rate is significantly reduced in the urothelium-specific *Eed* mutants during acute, chronic, and severe infections—consistent with the previous observation that *Ezh2* expression is closely associated with cell proliferation during bladder urothelial development.[23] Pathway analysis of the differentially expressed genes in the bladder urothelium between Eed^{cKO} mice and controls suggests that activity of the *p53* tumor suppression pathway is significantly elevated in Eed^{cKO} mice. Consistent with these observations, conditional knockout of *Kdm6a*—a histone demethylase that catalyzes an opposing biochemical reaction of PRC2 methyltransferase—results in a significant decrease in the *p53* tumor suppressor pathway activity.[55] Moreover, loss of function of *Kdm6a* significantly increases bladder cancer risk.[55] Thus, the *PRC2/Kdm6a-p53* axis regulates urothelial progenitor cell proliferation and tumorigenesis. Collectively, the PRC2-dependent epigenetic program may play a dual role in urothelial progenitor cells: it exacerbates the inflammatory host response through the *NF-κB* signaling pathway and controls urothelial regeneration through the *p53* tumor suppressor pathway by promoting proliferation of basal progenitor cells and inhibiting differentiation of superficial cells.

In summary, the findings here suggest that UTIs induce the PRC2-dependent epigenetic program in the bladder urothelium, which exacerbates inflammation and proliferation at the expense of differentiation

and tissue homeostasis. We further show the potential of a non-antibiotic strategy by inhibiting the methyltransferase activity of PRC2 to ameliorate UTIs. This study also provides evidence of trained immunity in the bladder. Future studies are needed to examine: (1) whether immune and urothelial cells may share similar or divergent roles to modulate immunity, (2) whether and how the UTI-induced epigenetic reprograming can be reversed to reduce the risk of bladder diseases, (3) whether trained immunity contribute to chronic and recurrent UTIs, and (4) whether targeting *Ezh2* enzymatic activity may reduce the risk and/or mitigate UTIs in patients. Ultimately, our study offers a tangible road map to alleviate the clinical and financial burden of UTIs on patients and health-care providers alike.

Limitations of the study

It is possible that UTIs cause other epigenetic remodeling pathways besides the PRC2-dependent program. In order to understand the scope of epigenetic remodeling associated with UTIs, other candidate epigenetic regulators should be examined. Additionally, we used UTI female mouse models, which may not fully recapitulate human UTIs. Therefore, when considering the clinical relevance of this study, it is important to investigate whether PRC2 alone exacerbates inflammatory host response and define the long-term impact of PRC2 inhibition in both male and female patients with UTI.

STAR★METHODS

Detailed methods are provided in the online version of this paper and include the following:

- KEY RESOURCES TABLE
- RESOURCE AVAILABILITY
  - Lead contact
  - Materials availability
  - Data and code availability
- EXPERIMENTAL MODEL AND STUDY PARTICIPANT DETAILS
  - Genetically engineered and wild type mouse lines
  - *In vivo* mouse models and therapy
  - *In vitro* UTI89 mouse models and therapy
- METHOD DETAILS
  - Acute, chronic and severe UTI mouse models and therapeutic intervention
  - RNA isolation, RNA-seq and RT-qPCR
  - Chromatin immunoprecipitation assay (ChIP)
  - Histology, inflammation score and immunofluorescent staining
  - Bladder organoids
- QUANTIFICATION AND STATISTICAL ANALYSIS

SUPPLEMENTAL INFORMATION

Supplemental information can be found online at https://doi.org/10.1016/j.isci.2023.106925.

ACKNOWLEDGMENTS

We thank all members of the X.L. lab, particularly Drs. Satoshi Kaneko and Chao Yang for technical supports and helpful discussions. We appreciate Drs. Rosalyn Adam and Eric Greer for critical and insightful comments on the manuscripts. This work was supported by NIH/NIDDK, United States (R01DK110477, X.L.; U01DK131377, X.L.; U54DK104309, M. A.), NIH/NCI, United States (R21CA249701 and 1R01CA267108, X.L.), and NHLBI, United States (1R01HL136921, X.L.).

AUTHOR CONTRIBUTIONS

X.L., Z.B., and C.G. designed the research studies. C.G., M.Z., X.S., Z.B., and S.Z. conducted experiments and acquired data. X.L., C.M.L., C.G., Y.Z., M.A., and M.Z. analyzed data. X.L. wrote the manuscript with the help of C.M.L., C.G., Z.B., Y.Z., and M.A.

DECLARATION OF INTERESTS

The authors declare no competing interests.

INCLUSION AND DIVERSITY

We support inclusive, diverse, and equitable conduct of research.

Received: September 15, 2022
Revised: April 8, 2023
Accepted: May 15, 2023
Published: May 20, 2023

REFERENCES

1. Hooton, T.M., Scholes, D., Hughes, J.P., Winter, C., Roberts, P.L., Stapleton, A.E., Stergachis, A., and Stamm, W.E. (1996). A prospective study of risk factors for symptomatic urinary tract infection in young women. N. Engl. J. Med. *335*, 468–474. https://doi.org/10.1056/NEJM199608153350703.

2. Scholes, D., Hooton, T.M., Roberts, P.L., Stapleton, A.E., Gupta, K., and Stamm, W.E. (2000). Risk factors for recurrent urinary tract infection in young women. J. Infect. Dis. *182*, 1177–1182. https://doi.org/10.1086/315827.

3. O'Brien, V.P., Hannan, T.J., Schaeffer, A.J., and Hultgren, S.J. (2015). Are you experienced? Understanding bladder innate immunity in the context of recurrent urinary tract infection. Curr. Opin. Infect. Dis. *28*, 97–105. https://doi.org/10.1097/QCO.0000000000000130.

4. Flores-Mireles, A.L., Walker, J.N., Caparon, M., and Hultgren, S.J. (2015). Urinary tract infections: epidemiology, mechanisms of infection and treatment options. Nat. Rev. Microbiol. *13*, 269–284. https://doi.org/10.1038/nrmicro3432.

5. Foxman, B. (2014). Urinary tract infection syndromes: occurrence, recurrence, bacteriology, risk factors, and disease burden. Infect. Dis. Clin. North Am. *28*, 1–13. https://doi.org/10.1016/j.idc.2013.09.003.

6. Hung, C.S., Dodson, K.W., and Hultgren, S.J. (2009). A murine model of urinary tract infection. Nat. Protoc. *4*, 1230–1243.

7. Thumbikat, P., Waltenbaugh, C., Schaeffer, A.J., and Klumpp, D.J. (2006). Antigen-specific responses accelerate bacterial clearance in the bladder. J. Immunol. *176*, 3080–3086.

8. Mora-Bau, G., Platt, A.M., van Rooijen, N., Randolph, G.J., Albert, M.L., and Ingersoll, M.A. (2015). Macrophages subvert adaptive immunity to urinary tract infection. PLoS Pathog. *11*, e1005044. https://doi.org/10.1371/journal.ppat.1005044.

9. Schwartz, D.J., Conover, M.S., Hannan, T.J., and Hultgren, S.J. (2015). Uropathogenic Escherichia coli superinfection enhances the severity of mouse bladder infection. PLoS Pathog. *11*, e1004599. https://doi.org/10.1371/journal.ppat.1004599.

10. Lyon, D., Howard, E.B., and Montgomerie, J.Z. (1982). Increased severity of urinary tract infection and bacteremia in mice with urinary bladder injury induced by cyclophosphamide. Infect. Immun. *38*, 558–562.

11. Hannan, T.J., Mysorekar, I.U., Hung, C.S., Isaacson-Schmid, M.L., and Hultgren, S.J. (2010). Early severe inflammatory responses to uropathogenic E. coli predispose to chronic and recurrent urinary tract infection. PLoS Pathog. *6*, e1001042. https://doi.org/10.1371/journal.ppat.1001042.

12. O'Brien, V.P., Hannan, T.J., Yu, L., Livny, J., Roberson, E.D.O., Schwartz, D.J., Souza, S., Mendelsohn, C.L., Colonna, M., Lewis, A.L., and Hultgren, S.J. (2016). A mucosal imprint left by prior Escherichia coli bladder infection sensitizes to recurrent disease. Nat. Microbiol. *2*, 16196. https://doi.org/10.1038/nmicrobiol.2016.196.

13. Hamon, M.A., Batsché, E., Régnault, B., Tham, T.N., Seveau, S., Muchardt, C., and Cossart, P. (2007). Histone modifications induced by a family of bacterial toxins. Proc. Natl. Acad. Sci. USA *104*, 13467–13472. https://doi.org/10.1073/pnas.0702729104.

14. Pereira, J.M., Hamon, M.A., and Cossart, P. (2016). A lasting impression: epigenetic memory of bacterial infections? Cell Host Microbe *19*, 579–582. https://doi.org/10.1016/j.chom.2016.04.012.

15. van der Heijden, C.D.C.C., Noz, M.P., Joosten, L.A.B., Netea, M.G., Riksen, N.P., and Keating, S.T. (2018). Epigenetics and trained immunity. Antioxid. Redox Signal. *29*, 1023–1040. https://doi.org/10.1089/ars.2017.7310.

16. Zheng, Y., Tipton, J.D., Thomas, P.M., Kelleher, N.L., and Sweet, S.M.M. (2014). Site-specific human histone H3 methylation stability: fast K4me3 turnover. Proteomics *14*, 2190–2199. https://doi.org/10.1002/pmic.201400060.

17. Zenk, F., Loeser, E., Schiavo, R., Kilpert, F., Bogdanović, O., and Iovino, N. (2017). Germ line-inherited H3K27me3 restricts enhancer function during maternal-to-zygotic transition. Science *357*, 212–216. https://doi.org/10.1126/science.aam5339.

18. Zee, B.M., Levin, R.S., Xu, B., LeRoy, G., Wingreen, N.S., and Garcia, B.A. (2010). In vivo residue-specific histone methylation dynamics. J. Biol. Chem. *285*, 3341–3350. https://doi.org/10.1074/jbc.M109.063784.

19. Ting, K., Aitken, K.J., Penna, F., Samiei, A.N., Sidler, M., Jiang, J.X., Ibrahim, F., Tolg, C., Delgado-Olguin, P., Rosenblum, N., and Bägli, D.J. (2016). Uropathogenic E. coli (UPEC) infection induces proliferation through enhancer of zeste homologue 2 (EZH2). PLoS One *11*, e0149118. https://doi.org/10.1371/journal.pone.0149118.

20. Cao, R., Wang, L., Wang, H., Xia, L., Erdjument-Bromage, H., Tempst, P., Jones, R.S., and Zhang, Y. (2002). Role of histone H3 lysine 27 methylation in Polycomb-group silencing. Science *298*, 1039–1043. https://doi.org/10.1126/science.1076997.

21. Kuzmichev, A., Nishioka, K., Erdjument-Bromage, H., Tempst, P., and Reinberg, D. (2002). Histone methyltransferase activity associated with a human multiprotein complex containing the Enhancer of Zeste protein. Genes Dev. *16*, 2893–2905. https://doi.org/10.1101/gad.1035902.

22. Müller, J., Hart, C.M., Francis, N.J., Vargas, M.L., Sengupta, A., Wild, B., Miller, E.L., O'Connor, M.B., Kingston, R.E., and Simon, J.A. (2002). Histone methyltransferase activity of a Drosophila Polycomb group repressor complex. Cell *111*, 197–208.

23. Guo, C., Balsara, Z.R., Hill, W.G., and Li, X. (2017). Stage- and subunit-specific functions of polycomb repressive complex 2 in bladder urothelial formation and regeneration. Development *144*, 400–408. https://doi.org/10.1242/dev.143958.

24. Balsara, Z.R., and Li, X. (2017). Sleeping beauty: awakening urothelium from its slumber. Am. J. Physiol. Renal Physiol. *312*, F732–F743. https://doi.org/10.1152/ajprenal.00337.2016.

25. Tan, J., Yang, X., Zhuang, L., Jiang, X., Chen, W., Lee, P.L., Karuturi, R.K.M., Tan, P.B.O., Liu, E.T., and Yu, Q. (2007). Pharmacologic disruption of Polycomb-repressive complex 2-mediated gene repression selectively induces apoptosis in cancer cells. Genes Dev. *21*, 1050–1063. https://doi.org/10.1101/gad.1524107.

26. Pasini, D., Bracken, A.P., Jensen, M.R., Lazzerini Denchi, E., and Helin, K. (2004). Suz12 is essential for mouse development and for EZH2 histone methyltransferase activity. EMBO J. *23*, 4061–4071. https://doi.org/10.1038/sj.emboj.7600402.

27. Hopkins, W.J., Gendron-Fitzpatrick, A., Balish, E., and Uehling, D.T. (1998). Time course and host responses to Escherichia coli urinary tract infection in genetically distinct mouse strains. Infect. Immun. *66*, 2798–2802.

28. Liu, Y., Mémet, S., Saban, R., Kong, X., Aprikian, P., Sokurenko, E., Sun, T.T., and Wu, X.R. (2015). Dual ligand/receptor interactions activate urothelial defenses against

uropathogenic E. coli. Sci. Rep. *5*, 16234. https://doi.org/10.1038/srep16234.

29. O'Brien, V.P., Dorsey, D.A., Hannan, T.J., and Hultgren, S.J. (2018). Host restriction of Escherichia coli recurrent urinary tract infection occurs in a bacterial strain-specific manner. PLoS Pathog. *14*, e1007457. https://doi.org/10.1371/journal.ppat.1007457.

30. Wu, J., Hayes, B.W., Phoenix, C., Macias, G.S., Miao, Y., Choi, H.W., Hughes, F.M., Jr., Todd Purves, J., Lee Reinhardt, R., and Abraham, S.N. (2020). A highly polarized TH2 bladder response to infection promotes epithelial repair at the expense of preventing new infections. Nat. Immunol. *21*, 671–683. https://doi.org/10.1038/s41590-020-0688-3.

31. Chan, C.Y., St John, A.L., and Abraham, S.N. (2013). Mast cell interleukin-10 drives localized tolerance in chronic bladder infection. Immunity *38*, 349–359. https://doi.org/10.1016/j.immuni.2012.10.019.

32. Hannan, T.J., Roberts, P.L., Riehl, T.E., van der Post, S., Binkley, J.M., Schwartz, D.J., Miyoshi, H., Mack, M., Schwendener, R.A., Hooton, T.M., et al. (2014). Inhibition of cyclooxygenase-2 prevents chronic and recurrent cystitis. EBioMedicine *1*, 46–57. https://doi.org/10.1016/j.ebiom.2014.10.011.

33. Vermeulen, S.H., Hanum, N., Grotenhuis, A.J., Castaño-Vinyals, G., van der Heijden, A.G., Aben, K.K., Mysorekar, I.U., and Kiemeney, L.A. (2015). Recurrent urinary tract infection and risk of bladder cancer in the Nijmegen bladder cancer study. Br. J. Cancer *112*, 594–600. https://doi.org/10.1038/bjc.2014.601.

34. Knutson, S.K., Wigle, T.J., Warholic, N.M., Sneeringer, C.J., Allain, C.J., Klaus, C.R., Sacks, J.D., Raimondi, A., Majer, C.R., Song, J., et al. (2012). A selective inhibitor of EZH2 blocks H3K27 methylation and kills mutant lymphoma cells. Nat. Chem. Biol. *8*, 890–896.

35. Kim, K.H., and Roberts, C.W.M. (2016). Targeting EZH2 in cancer. Nat. Med. *22*, 128–134. https://doi.org/10.1038/nm.4036.

36. Mullenders, J., de Jongh, E., Brousali, A., Roosen, M., Blom, J.P.A., Begthel, H., Korving, J., Jonges, T., Kranenburg, O., Meijer, R., and Clevers, H.C. (2019). Mouse and human urothelial cancer organoids: a tool for bladder cancer research. Proc. Natl. Acad. Sci. USA *116*, 4567–4574. https://doi.org/10.1073/pnas.1803595116.

37. Lee, S.T., Li, Z., Wu, Z., Aau, M., Guan, P., Karuturi, R.K.M., Liou, Y.C., and Yu, Q. (2011). Context-specific regulation of NF-kappaB target gene expression by EZH2 in breast cancers. Mol. Cell *43*, 798–810. https://doi.org/10.1016/j.molcel.2011.08.011.

38. Iannetti, A., Ledoux, A.C., Tudhope, S.J., Sellier, H., Zhao, B., Mowla, S., Moore, A., Hummerich, H., Gewurz, B.E., Cockell, S.J., et al. (2014). Regulation of p53 and Rb links the alternative NF-kappaB pathway to EZH2 expression and cell senescence. PLoS Genet. *10*, e1004642. https://doi.org/10.1371/journal.pgen.1004642.

39. Naik, S., Larsen, S.B., Gomez, N.C., Alaverdyan, K., Sendoel, A., Yuan, S., Polak, L., Kulukian, A., Chai, S., and Fuchs, E. (2017). Inflammatory memory sensitizes skin epithelial stem cells to tissue damage. Nature *550*, 475–480. https://doi.org/10.1038/nature24271.

40. Ordovas-Montanes, J., Dwyer, D.F., Nyquist, S.K., Buchheit, K.M., Vukovic, M., Deb, C., Wadsworth, M.H., 2nd, Hughes, T.K., Kazer, S.W., Yoshimoto, E., et al. (2018). Allergic inflammatory memory in human respiratory epithelial progenitor cells. Nature *560*, 649–654. https://doi.org/10.1038/s41586-018-0449-8.

41. Wiles, T.J., Dhakal, B.K., Eto, D.S., and Mulvey, M.A. (2008). Inactivation of host Akt/protein kinase B signaling by bacterial pore-forming toxins. Mol. Biol. Cell *19*, 1427–1438. https://doi.org/10.1091/mbc.E07-07-0638.

42. Zhang, Z., Wang, M., Eisel, F., Tchatalbachev, S., Chakraborty, T., Meinhardt, A., and Bhushan, S. (2016). Uropathogenic Escherichia coli epigenetically manipulate host cell death pathways. J. Infect. Dis. *213*, 1198–1207. https://doi.org/10.1093/infdis/jiv569.

43. Netea, M.G., Quintin, J., and van der Meer, J.W.M. (2011). Trained immunity: a memory for innate host defense. Cell Host Microbe *9*, 355–361. https://doi.org/10.1016/j.chom.2011.04.006.

44. Lau, C.M., and Sun, J.C. (2018). The widening spectrum of immunological memory. Curr. Opin. Immunol. *54*, 42–49. https://doi.org/10.1016/j.coi.2018.05.013.

45. Netea, M.G., Schlitzer, A., Placek, K., Joosten, L.A.B., and Schultze, J.L. (2019). Innate and adaptive immune memory: an evolutionary continuum in the host's response to pathogens. Cell Host Microbe *25*, 13–26. https://doi.org/10.1016/j.chom.2018.12.006.

46. Mysorekar, I.U., and Hultgren, S.J. (2006). Mechanisms of uropathogenic Escherichia coli persistence and eradication from the urinary tract. Proc. Natl. Acad. Sci. USA *103*, 14170–14175.

47. Olson, P.D., and Hunstad, D.A. (2016). Subversion of host innate immunity by uropathogenic Escherichia coli. Pathogens *5*, 2. https://doi.org/10.3390/pathogens5010002.

48. Mulvey, M.A., Lopez-Boado, Y.S., Wilson, C.L., Roth, R., Parks, W.C., Heuser, J., and Hultgren, S.J. (1998). Induction and evasion of host defenses by type 1-piliated uropathogenic Escherichia coli. Science *282*, 1494–1497.

49. Justice, S.S., Hung, C., Theriot, J.A., Fletcher, D.A., Anderson, G.G., Footer, M.J., and Hultgren, S.J. (2004). Differentiation and developmental pathways of uropathogenic Escherichia coli in urinary tract pathogenesis. Proc. Natl. Acad. Sci. USA *101*, 1333–1338.

50. Justice, S.S., Hunstad, D.A., Seed, P.C., and Hultgren, S.J. (2006). Filamentation by Escherichia coli subverts innate defenses during urinary tract infection. Proc. Natl. Acad. Sci. USA *103*, 19884–19889.

51. Klumpp, D.J., Weiser, A.C., Sengupta, S., Forrestal, S.G., Batler, R.A., and Schaeffer, A.J. (2001). Uropathogenic Escherichia coli potentiates type 1 pilus-induced apoptosis by suppressing NF-kappaB. Infect. Immun. *69*, 6689–6695. https://doi.org/10.1128/IAI.69.11.6689-6695.2001.

52. Hunstad, D.A., Justice, S.S., Hung, C.S., Lauer, S.R., and Hultgren, S.J. (2005). Suppression of bladder epithelial cytokine responses by uropathogenic Escherichia coli. Infect. Immun. *73*, 3999–4006. https://doi.org/10.1128/IAI.73.7.3999-4006.2005.

53. Billips, B.K., Forrestal, S.G., Rycyk, M.T., Johnson, J.R., Klumpp, D.J., and Schaeffer, A.J. (2007). Modulation of host innate immune response in the bladder by uropathogenic Escherichia coli. Infect. Immun. *75*, 5353–5360. https://doi.org/10.1128/IAI.00922-07.

54. Gur, C., Coppenhagen-Glazer, S., Rosenberg, S., Yamin, R., Enk, J., Glasner, A., Bar-On, Y., Fleissig, O., Naor, R., Abed, J., et al. (2013). Natural killer cell-mediated host defense against uropathogenic E. coli is counteracted by bacterial hemolysinA-dependent killing of NK cells. Cell Host Microbe *14*, 664–674. https://doi.org/10.1016/j.chom.2013.11.004.

55. Kaneko, S., and Li, X. (2018). X chromosome protects against bladder cancer in females via a KDM6A-dependent epigenetic mechanism. Sci. Adv. *4*, eaar5598. https://doi.org/10.1126/sciadv.aar5598.

56. Hu, C.C.A., Liang, F.X., Zhou, G., Tu, L., Tang, C.H.A., Zhou, J., Kreibich, G., and Sun, T.T. (2005). Assembly of urothelial plaques: tetraspanin function in membrane protein trafficking. Mol. Biol. Cell *16*, 3937–3950. https://doi.org/10.1091/mbc.E05-02-0136.

STAR★METHODS

KEY RESOURCES TABLE

REAGENT or RESOURCE	SOURCE	IDENTIFIER
Antibodies		
Rabbit Polyclonal anti-H3K27me3	Millipore	Cat#07-449
Rabbit Polyclonal anti-H3K4me3	Motif Active	Cat#39159
Normal Rabbit IgG	Cell Signaling Technology	Cat#2729
Rabbit monoclonal Anti- Ezh2 [D2C9]	Cell Signaling Technology	Cat#5246
Rabbit monoclonal Anti- Ki67 [SP6]	Abcam	Cat#16667
Rabbit Polyclonal Anti-pHH3	Millipore	Cat#06-570
Rabbit polyclonal Anti-Krt5-1	Abcam	Cat#ab53121
Chicken polyclonal Anti-Krt5-2	Covance	Cat#SIG-3475
Mouse monoclonal Anti- Upk3a [AU1]	Sun et al.[56]	N/A
Mouse monoclonal Anti-Krt20 [Clone Ks20.8]	Dako	Cat#M7019
Mouse monoclonal Anti- IκBα[L35A5]	Cell Signaling Technology	Cat#4814
Mouse monoclonal Anti- RelA/p65 [F-6]	Santa Cruz Biotechnology	Cat#sc8008
Bacterial and Virus Strains		
UTI89	Hultgren et al.[6]	N/A
Chemicals, peptides, and recombinant proteins		
EPZ005687 (*in vivo* 2.5 mg/kg; cell culture 10 mM)	APExBIO	Cat# A4171
DZNep (1.5 mg/kg)	Selleckchem	Cat# S7120
CPP (300 mg/kg)	Sigma-Aldrich	Cat# C7397
Recombinant Human KGF/FGF-7 Protein	R&D Systems	Cat# 251-KG
Recombinant Human FGF-10 Protein	R&D Systems	Cat# 345-FG
Y-27632 (hydrochloride)	Cayman Chemical	Cat# 10005583
A 83-01	Sigma-Aldrich	Cat# Sml0788-5mg
Critical Commercial Assays		
Protein G Dynabeads	Invitrogen	Cat# 10003D
RNeasy RNA isolation kit	Qiagen	Cat# 74034
Super-Script® III Reverse Transcriptase Kit	Invitrogen	Cat# 18080051
FastStart™ SYBR® Green Master mix (ROX)	Roche	Cat# 4913914001
Deposited Data		
RNAseq DEG for UTI vs. PBS	This paper	GEO: GSE228414
RNAseq DEG for Eed^{cKO} vs. WT in CPP	This paper	GEO: GSE228422
Experimental Models: Organisms/Strains		
B6; 129S1-Eedtm1Sho/J	The Jackson Laboratory	022727
C57BL/6J (7-8weeks, female)	The Jackson Laboratory	000664
C3H/HeNCrl (7-8weeks, female)	Charles River	025
Oligonucleotides		
Primers for ChIP DNA and qRT-PCR, see Table S2	This paper	N/A

RESOURCE AVAILABILITY

Lead contact

Inquiries for additional information or requests related to experimental details and reagents should communicate with the lead contact, Xue Li (sean.li@cshs.org).

Materials availability

This study did not generate new unique reagents.

Data and code availability

- RNA-seq data have been deposited at GEO and are publicly available as of the date of publication. Accession numbers are listed in the key resources table. Original histological and immunofluorescent stained as well as urine and tissue bacterial counts reported in this paper will be shared by the lead contact upon request.
- This paper does not report original code.
- Any additional information required to reanalyze the data reported in this paper is available from the lead contact upon request.

EXPERIMENTAL MODEL AND STUDY PARTICIPANT DETAILS

Genetically engineered and wild type mouse lines

Mouse line *Eed*$^{F/F}$;*Upk2*^{Cre} was derived from mating *Eed* floxed allele with *Upk2* promoter-driven *Cre* transgenic allele.[23] C57BL/6J mice (#000664, female, 7-8 week-old) were obtained from The Jackson Laboratory. C3H/HeNCrl mice (#025, female, 7-8 week-old) were obtained from Charles River. All animal studies were performed according to protocols reviewed and approved by the Institutional Animal Care and Use Committee at Boston Children's Hospital and Cedars-Sinai Medical Center. All protocols for animal studies followed ARRIVE guidelines.

In vivo mouse models and therapy

In vivo acute UTI mouse models were recapitulated by inoculating a human UPEC strain UTI89 (50 μL of 10^8 colony forming units (CFU) in PBS) directly into the bladder of C57Bl/6J mice (female, 7-8 week-old).[6] UTI89 strain was generously provided by Dr. Scott Hultgren (Washington University, St. Louis, USA). Non-antibiotic therapeutic treatment, EPZ005687 (2.5 mg/kg, APExBIO, A4171) and DZNep (1.5 mg/kg, Selleckchem, S7120), were administered via intraperitoneal injection to wild type mice modeled for chronic cystitis and C^+UTI superinfection; EPZ005687 is a Ezh2-specific inhibitor and DZNep is a non-specific Ezh2 inhibitor.

In vitro UTI89 mouse models and therapy

In vitro infection was recapitulated by adding UTI89 (~1 × 10^7 CFU/mL, 1 h) for 1 h to differentiated organoids, followed by PBS wash and immunofluorescent staining. To examine the role of Ezh2, we pretreated differentiated organoids with 10 μM EPZ005687 for 1 h prior to infection. Primary cells used to generate organoids were from female mice and cultured at conditions of 37°C and 5% CO_2.

METHOD DETAILS

Acute, chronic and severe UTI mouse models and therapeutic intervention

We recapitulated three forms of UTIs in mice—acute, chronic, and severe UTIs. For acute infections, mice were infected once with UTI89 (50 μL of 10^8 CFU in PBS).[6] For chronic infections, C57Bl6 mice were infected 7 times with 7 days of convalescence between each infection. For severe infections, we injected a single dose of cyclophosphamide (CPP, 300 mg/kg, Sigma C7397, intraperitoneal (i.p.) injection) 1 day prior to UTI89 inoculation (50 μL of 10^8 CFU of UTI89). CPP treatment makes the bladder susceptible to a severe outcome upon UTI89 inoculation[10]; thus we referred to this severe UTI infection model as a C^+UTI superinfection. Urine bacterial burden was determined by serially diluting urine samples to measure CFU; CFU was normalized by urine volume. Controls were inoculated with phosphate buffered saline (PBS) instead of UTI89. To test pharmacological efficacy of Ezh2 inhibitors on chronic cystitis, we inoculated C3H/HeNCrl mice with 10^9 CFU of UTI89 and administered treatment.[12] We did not administer Ezh2 inhibitors to

C57Bl6 mice modeling acute infections using because these mice spontaneously resolve from acute infections.

RNA isolation, RNA-seq and RT-qPCR

RNeasy RNA isolation kit (Qiagen) was used to isolate total RNA from micro-dissected bladder urothelium. Briefly, mouse bladder was harvested and placed immediately in cold autoclaved PBS. Under stereo dissecting microscope, the bladder was bisected to expose the lumen. With one forceps holding and stabilizing the bladder at the muscular layer, the urothelium was gently peeled off using another forceps. This process usually took less than 2 min. Genomic DNA was removed using gDNA Eliminator spin columns (Qiagen). Illumina 2500 was used for RNA-seq (20M, PE150). Cutoff for differentially expressed genes (DEGs) was based on *padj* < 0.05 and more than 2-fold changes. Pathway analysis was done using the Ingenuity Pathway Analysis (IPA) software package (Qiagen). For quantitative real-time PCR (qRT-PCR) experiments, mRNA was reverse-transcribed into cDNA using the Super-Script III Reverse Transcriptase Kit (Invitrogen). qRT-PCR analyses were performed using SYBR Green (Roche) on an ABI-7500 detector (Applied BioSystems). Relative gene expression levels were normalized to the internal control *Gapdh*. Gene-specific primers were listed in Table S2. All experiments were done at room temperature.

Chromatin immunoprecipitation assay (ChIP)

Micro-dissected urothelial cells from 20 bladders per group were crosslinked with 1% formaldehyde at room temperature for 15 min.[23] Cells were then lysed and sonicated to an average size of 500–1000 base pairs. Immunoprecipitation of chromatin lysates was performed using 1 μg per reaction of the following antibodies: anti-H3K27me3 (Millipore, 07–449), anti-H3K4me3 (Motif Active, 39159), or control IgG. Immunoprecipitates were collected with Protein G Dynabeads (Invitrogen) and protein/DNA crosslinks were reversed with 5M NaCl. DNA was purified and ChIP DNA was analyzed by quantitative PCR using the following *IκBα* locus-specific primers, −10 kb region: forward, 5′TAA AGC ACA TGT GTG GGG TCT C; reverse, 5′ATC GAA CAT AGG GCC ATG AGA G; −0.3 kb region: forward, 5′CAT CGG AGA AAC TCC CTG CG; reverse, 5′CAA ACC AAA ATC GCC CGG TG (Table S2). Each sample was normalized using input DNA.

Histology, inflammation score and immunofluorescent staining

Standard hematoxylin and eosin staining (H&E) was used for histological analysis. Inflammatory score were determined using the described criteria[27]: (0) Normal; (1) Inflammatory cell infiltration in lamina propria layer (focal); (2) Edema and inflammatory cell infiltration (diffuse); (3) Marked inflammatory cells with necrosis and neutrophils in and on bladder urothelium; (4) Inflammatory cells infiltration extends into muscle in addition to criteria for grade 3; (5) Loss of surface epithelium (necrosis with full-thickness inflammatory cell infiltration). Inflammation scores were determined independently by three individuals, analyzed using Student's *t* test, and $p < 0.05$ was considered significant. To quantify infiltration of neutrophils, we used at least four bladders per experimental group. Exact sample numbers are indicated in the figure legend. Three paraffin sections from each of the bladders were H&E stained. Neutrophils were identified based on their characteristic multilobed nucleus morphology under a 200X microscopic lens. Percent of neutrophils of tptotal cells was calculated and analyzed using Student's *t* test and $p < 0.05$ was considered significant. Antibodies used for immunofluorescent staining included Ezh2 (1:100 Cell signaling, 5246), H3K27me3 (1:100 Millipore 07–449), Ki67 (1:100 Abcam 16667), pHH3 (1:100 Millipore, 06–570), Krt5 (1:500 Abcam, ab53121; 1:500, Covance, SIG-3475), Upk3a (1:200 provided by Dr. T.T. Sun), Krt20 (1:50, Dako, M7019), IκBα (1:100 Cell signaling, 4814) and RelA/p65 (1:100, Santa Cruz, sc8008). Images were captured using a ZEISS fluorescence microscope. Histological and immunostaining images represent more than three biology replicates.

Bladder organoids

Mouse (female C57Bl6, 7–8 weeks old) bladder mucosa was digested with TrypLE (ThermoFisher) containing 10 mM Y-27632 (Sigma Aldrich) at 37°C for 1 h.[36] Cell suspension was cultured in basement membrane extract (BME, R&D Systems) in defined medium (Adv DMEM/F-12, 100 ng/mL FGF10, 25 ng/mL FGF7, 500 nM A83-01 and 2% B27) for a week. To differentiate bladder organoids to urothelial cells, organoids (100–200 μm in diameters) were differentiated in 2D culture in F-12 media on TC-treated glass coverslip (SolarBio) for one week without BME.

QUANTIFICATION AND STATISTICAL ANALYSIS

Student's *t* test was used to analyze datasets with normal distribution including qRT-PCR, cell proliferation and inflammatory scores. Nonparametric tests (Mann-Whitney) were used for results with nonnormal distribution such as bacterial colony forming units. Unpaired Student's *t* test and one-way ANOVA test were used in Figure 2E to compare multiple groups of data. In instances when sample size (n) is listed as greater than or equal to a value (e.g., $n \geq 17$; Figure 4B), experiments began with a greater number of mice (e.g., n = 33), but ended with less mice due to attrition (e.g., n = 17). All experiments were repeated more than three times to ensure reproducibility. Data is reported in the form of box and whisker plots with individual data points. The upper and lower limits of the box represent the third and first quartiles respectively; the line within the box indicates the median, and the whiskers extend toward maximum and minimum values. Graphs with three points (without box) indicate maximum value, median, and minimum value (from top to bottom). Boxes are not shown for datasets with only 3 values. For all tests, $p < 0.05$ is considered statistically significant.